

Classification of dark states in multilevel dissipative systemsDaniel Finkelstein-Shapiro,^{1,*} Simone Felicetti,² Thorsten Hansen,³ Tõnu Pullerits,¹ and Arne Keller^{2,4,†}¹*Division of Chemical Physics, Lund University, Box 124, 221 00 Lund, Sweden*²*Laboratoire Matériaux et Phénomènes Quantiques, Université Paris Diderot, CNRS UMR 7162, 75013, Paris, France*³*Department of Chemistry, University of Copenhagen, DK 2100 Copenhagen, Denmark*⁴*Université Paris-Sud, 91405 Orsay, France*

(Received 19 October 2018; revised manuscript received 3 March 2019; published 20 May 2019)

Dark states are eigenstates or steady states of a system that are decoupled from the radiation. Their use, along with associated techniques such as stimulated Raman adiabatic passage, has extended from atomic physics, where it is an essential cooling mechanism, to more recent versions in the condensed phase where it can increase the coherence times of qubits. These states are often discussed in the context of unitary evolution and found with elegant methods exploiting symmetries, or via the Morris-Shore transformation. However, the link with dissipative systems is not always transparent, and distinctions between classes of coherent population trapping are not always clear. We present a detailed overview of the arguments to find stationary dark states in dissipative systems, and examine their dependence on the Hamiltonian parameters, their multiplicity, and purity. We evidence the class of dark states that depends not only on the detunings of the lasers but also on their relative intensities and phases. We illustrate the criteria with the more complex physical system of the hyperfine transitions of ⁸⁷Rb and show how a knowledge of the dark-state manifold can guide the preparation of pure states.

DOI: [10.1103/PhysRevA.99.053829](https://doi.org/10.1103/PhysRevA.99.053829)**I. INTRODUCTION**

The concept of dark states is at the heart of various atomic and optical processes. The most important are coherent population trapping (CPT) [1,2], electromagnetically induced transparency (EIT) [3,4], and stimulated Raman adiabatic passage (STIRAP) [5]. These three processes have been most studied in the so-called Λ three-level atomic systems, consisting of two ground states and one excited state. The two ground-excited transitions can be independently driven by coherent laser fields. In such Λ systems, the dark state consists of a coherent superposition of both ground states, which is not coupled to the excited state. Hence, the atom in a dark state can neither absorb nor emit light, hence its name.

In CPT, it is the optical pumping which, through spontaneous emission, will populate the dark state. The EIT process can be seen as the direct manifestation of the dark state since once the atoms constituting the medium have been completely pumped to the dark state, the medium becomes transparent. The CPT and EIT processes are generally considered in a stationary regime, whereas for the STIRAP process, both laser fields are pulsed in such a way as to adiabatically transfer the population from one of the ground states to the other. The STIRAP process can be seen as an adiabatic following of the instantaneous dark state of the Hamiltonian [6].

Originating in atomic and molecular physics [7,8], the preparation of dark states has been exploited for several purposes. It is extensively used for atomic cooling [9–11]

by means of the temperature-dependent Doppler shift. Using counterpropagating laser beams, the necessary detuning condition that both lasers must fulfill for the existence of a dark state is only fulfilled by atoms with no velocity component in the propagation direction of the laser beams. Optical pumping will thus populate the dark state corresponding to these zero-velocity atoms.

In metrology, CPT can be incorporated in a variant of Ramsey interferometry where it provides the notable advantages of replacing magnetic fields and microwave pumping by optical pumping [12–14]. Recently, the preparation of an initial dark state was used to obtain a lower limit for the electric dipole moment of the electron [15].

It has been used for testing QED and extended to state initialization in quantum information [16,17] including qubit gates, on solid-state systems such as spin systems in nitrogen vacancies [18], in superconducting circuits [19], and in semiconductor heterostructures [20–23]. Using CPT, the coherence lifetimes of qubits have been successfully extended by orders of magnitude [24,25]. Some recent proposals suggest its use in plasmonic systems [26]. Multiple-level systems are also quite common in atomic and solid-state devices [5,17,24,25,27–29].

There are two viewpoints of dark states depending on whether dissipation processes are included or not. In a Hamiltonian system with unitary evolution, coherent superposition of the ground states decouples from a radiation field provided some conditions are met for the field frequencies. In a dissipative system, this superposition becomes the stationary state regardless of the initial conditions.

In order to find the possible dark states an atomic or molecular system can support, various approaches have been

*daniel.finkelstein_shapiro@chemphys.lu.se

†arne.keller@u-psud.fr

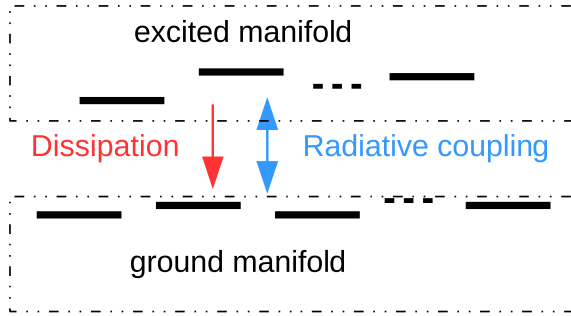


FIG. 1. N -level system consisting of a ground-state manifold coupled radiatively to an excited-state manifold. The excited state can also relax dissipatively to the ground state.

followed. An analysis based on symmetries and constants of the motion has permitted the generalization to multilevel systems, as long as the system preserves some symmetries notably with respect to the decouplings [30,31]. The Morris-Shore (MS) transformation separates a set of N_g degenerate ground states and N_e degenerate excited states into pairs of bright states, dark states, and spectator states [32–34], recently extended to the case of small detunings [35]. The transformation relies on having a number of ground states in excess in order to result in dark states. There are other instances, however, where certain states might decouple from the radiation that fall outside of these considered cases (for example, for an equal number of ground and excited states).

Beyond the symmetry considerations and MS transformation, it is common to calculate numerically the time evolution of the density matrix equations using a Lindblad operator as the generator of the dynamics. As such, dark states can be confirmed and their departure thereof studied whenever, for example, ground-state decoherence is present. However, such a numerical approach can sometimes miss some of the dark-state conditions at the same time that it fails to provide a comprehensive framework such as the MS transformation provides in the case of spectator states. As such a more direct and more efficient method to find dark states is desired. Furthermore, given the recent clarifications on the properties of dissipative steady states [36]—their unicity and purity—a review of dark states in light of these advances is needed.

In this work, we give an overview for the conditions to find dark states in dissipative systems whose dynamics is described by a Lindblad equation [37,38], and systematically study the multiplicity of dark stationary states, their purity, and their dependence on laser field detunings and Rabi frequencies.

II. GENERAL CONSIDERATIONS

A. System and definitions

We consider an N -level system which can be divided into N_g ground states $|g_i\rangle$ with energy $E_i^{(g)}$ ($i = 1, 2, \dots, N_g$), and $N_e = N - N_g$ excited states $|e_j\rangle$ with energy $E_j^{(e)}$ ($j = 1, 2, \dots, N_e$), that decay to the ground states via spontaneous emission or coupling to a bath, at rate γ_{ij} (see Fig. 1). The

Hamiltonian of the system can be written as

$$H(t) = \sum_{i=1}^{N_g} E_i^{(g)} |g_i\rangle\langle g_i| + \sum_{j=1}^{N_e} E_j^{(e)} |e_j\rangle\langle e_j| + \sum_{i,j} F_{ij}(t) (|g_i\rangle\langle e_j| + |e_j\rangle\langle g_i|), \quad (1)$$

where $F_{ij}(t) = 2F_{ij} \cos(\omega_{ij}t + \phi_{ij})$ represent the coherent laser beams with frequencies ω_{ij} coupling the manifold of ground states to the manifolds of excited states.

We restrict our attention to the case where each transition $g_i \leftrightarrow e_j$ is driven by at most one laser, so that the problem can be reduced to a time-independent one (see Appendix A). We assume no spectral overlap between the transitions.

We suppose that there exists an interaction picture such that in the rotating-wave approximation (RWA) the system evolution is described by a Lindblad equation [37,38] $\dot{\rho} = L\rho$, with a time-independent Lindblad operator L . The operator L can be written as

$$L(\rho) = -i[H, \rho] + \sum_{\{ij\}} \gamma_{ij} D_{ij}(\rho). \quad (2)$$

We set $\hbar = 1$ throughout the paper, and consider that energy and frequency are equivalent. The Hamiltonian H is now time independent and can be written in terms of the operators $\sigma_{ij}^z = |g_i\rangle\langle g_i| - |e_j\rangle\langle e_j|$ (see Appendix A) as

$$H = \sum_{i=1}^{N_g} \sum_{j=1}^{N_e} [\Delta_{ij} \sigma_{ij}^z + (V_{ij} |g_i\rangle\langle e_j| + \text{H.c.})], \quad (3)$$

where $V_{ij} = F_{ij} e^{i\phi_{ij}}$ are the complex Rabi frequencies and

$$\Delta_{ij} = E_j^{(e)} - E_i^{(g)} - \omega_{ij} \quad (4)$$

is the detuning between the atomic transition energy $E_j^{(e)} - E_i^{(g)}$ and the laser frequency ω_{ij} . $\gamma_{ij} D_{ij}(\rho)$ describes the decay of excited state $|e_j\rangle$ to ground state $|g_i\rangle$. According to the Lindblad equation [37,38],

$$D_{ij}(\rho) = -\frac{1}{2} \{\sigma_{ij}^\dagger \sigma_{ij}, \rho\} + \sigma_{ij} \rho \sigma_{ij}^\dagger, \quad (5)$$

where $\{A, B\}$ is the anticommutator of A and B and $\sigma_{ij} = |g_i\rangle\langle e_j|$.

We show in Appendix A that in the RWA this time-independent formulation is possible if and only if there is at most one laser coupling associated to each transition $g_i \leftrightarrow e_j$, as we have mentioned above, but also if, to each such coupled transition, we can assign two real numbers ϵ_i, ϵ_j such that

$$\epsilon_i - \epsilon_j = \omega_{ij}. \quad (6)$$

This condition cannot always be met for arbitrary frequencies and can impose a relation between the laser frequencies.

There are also important cases of interest where control fields are added within the ground or excited manifolds. These can be resolved by block-diagonalizing them and redefining the ground states $|g_i\rangle$ or excited states $|e_j\rangle$ so that the problem is brought back to the desired form. Some of these schemes have been shown to be desirable, for example, in the acceleration of cooling of trapped ions [39–42].

B. General conditions for the existence of dark states

We say that a stationary state is dark when it involves only the ground-state manifold (there is no population in the excited states). In general the steady state has nonzero density on both the ground-state $\{|g_i\rangle\}$ and excited-state $\{|e_j\rangle\}$ manifolds, and only fulfills the conditions of dark states for specific values of the parameters. The problem of tuning to dark states consists in finding the set of parameters, that is, the laser intensities and frequencies, for which the steady state belongs to the ground-state manifold $\{|g_i\rangle\}$.

It is convenient to rewrite the Lindblad operator as a non-Hermitian Hamiltonian part $L_{\tilde{H}}$, and a quantum jump operator J , as it has been written often, for example, in the study of blinking or quantum trajectory theory [43]:

$$L\rho = L_{\tilde{H}}\rho + J(\rho), \quad (7)$$

where $L_{\tilde{H}}\rho = -i(\tilde{H}\rho - \rho\tilde{H}^\dagger)$ with $\tilde{H} = H - i\Gamma$ with $\Gamma = \sum_{\{ij\}} \gamma_{ij}(\sigma_{ij}^\dagger\sigma_{ij})$ and $J(\rho) = \sum_{\{ij\}} \gamma_{ij}\sigma_{ij}\rho\sigma_{ij}^\dagger$.

Our general method to obtain the conditions for dark states relies on the following theorem.

Theorem 1. The N -level system whose evolution is governed by the Lindblad operator L given by Eq. (2) has a dark state ρ_d if and only if $L_{\tilde{H}}\rho_d = 0$.

In other words, a dark state is an eigenstate of $L_{\tilde{H}}$ with a zero eigenvalue. The proof is given in Appendix B; we just give the heuristic of the proof here. It is based on two observations:

(1) In general the eigenvalues of $L_{\tilde{H}}$ have a real part which is strictly negative, which is related to the fact that the eigenvalues of \tilde{H} have a strictly negative imaginary part due to the total decay rate $\sum_i \gamma_{ij}$ of excited states $\{|e_j\rangle\}$. The only way to have a zero eigenvalue is such that the corresponding eigenstate ρ_d has no component on these decaying excited states $\{|e_j\rangle\}$.

(2) If $L_{\tilde{H}}\rho_d = 0$ then also $L\rho_d = 0$ as the jump operator gives zero, $J(\rho_d) = 0$, on any state in the subspace spanned by $\{|g_i\rangle\}$.

In that way, when $L_{\tilde{H}}\rho_d = 0$, we ensure that the corresponding eigenvector is a steady state of L with no component in the excited states. Hence, it is a dark state. The reverse is also true: all dark state ρ_d fulfill $L_{\tilde{H}}\rho_d = 0$.

As dark states belong to the subspace spanned by the ground states only, it is thus convenient to define the projection operator on this subspace $P = \sum_{i=1}^{N_g} |g_i\rangle\langle g_i|$ and its orthogonal complement $Q = \mathbb{1} - P = \sum_{j=1}^{N_e} |e_j\rangle\langle e_j|$, where $\mathbb{1}$ is the identity operator in the Hilbert space \mathcal{H} spanned by the N states. We also define superprojectors \mathcal{P} and $\mathcal{Q} = \mathbb{1} - \mathcal{P}$, where here $\mathbb{1}$ means the identity operator on the Liouville space of linear operators on \mathcal{H} . These superprojectors act as superoperators in the following way: $\mathcal{P}\rho = P\rho P$ and $\mathcal{Q}\rho = P\rho Q + Q\rho P + Q\rho Q$.

By inserting the identity $\mathcal{P} + \mathcal{Q} = \mathbb{1}$ between $L_{\tilde{H}}$ and ρ in the equation $L_{\tilde{H}}\rho = 0$, and projecting the resulting equation with the two superprojectors, we obtain the following two equations:

$$\begin{aligned} \mathcal{P}L_{\tilde{H}}\mathcal{P}\rho + \mathcal{P}L_{\tilde{H}}\mathcal{Q}\rho &= 0, \\ \mathcal{Q}L_{\tilde{H}}\mathcal{P}\rho + \mathcal{Q}L_{\tilde{H}}\mathcal{Q}\rho &= 0. \end{aligned} \quad (8)$$

As dark states belong entirely to the ground-state manifold, we can enforce the condition $\mathcal{P}\rho = \rho$ and thus $\mathcal{Q}\rho = 0$. In Appendix C we show that using these conditions, Eqs. (8) become

$$[PHP, \rho] = 0, \quad (9)$$

$$QHP\rho = 0. \quad (10)$$

From the first equation, Eq. (9), we infer that there exists a common orthonormal basis of $P\mathcal{H}$ in which the matrix representation of ρ and PHP is diagonal. But PHP is diagonal in the $\{|g_i\rangle\}$ basis,

$$PHP = \sum_{i=1}^{N_g} \mathcal{E}_i |g_i\rangle\langle g_i|, \quad (11)$$

where we have defined [see Eqs. (3) and Eq. (4)]

$$\mathcal{E}_i = \sum_j \Delta_{ij}. \quad (12)$$

Therefore, if the PHP spectrum is nondegenerate then the only solutions to Eq. (9) are matrices ρ which are also diagonal in this basis. But this is a trivial solution and in this case Eq. (10) implies that $V_{ij} = 0$. Hence, nontrivial solutions can arise if and only if PHP has a degenerate spectrum. This degeneracy condition translates to a constraint on the laser frequencies. For instance, the requirement that two PHP eigenvalues are equal, $\mathcal{E}_i = \mathcal{E}_{i'}$, consists in a relation between the detunings $\sum_j (\Delta_{ij} - \Delta_{i'j}) = 0$ [by Eq. (12)], which translates into a relation between laser frequencies [see Eq. (4)].

Let us denote P_s , the orthogonal projectors on the eigensubspace of dimension d_s , associated to the $d_s - 1$ times degenerate eigenvalue \mathcal{E}_s . We have $\sum_s P_s = P$, $P_s P_{s'} = \delta_{ss'} P_s$, and $\sum_s d_s = N_g$. Then PHP can be written as

$$PHP = \sum_s \mathcal{E}_s P_s, \quad (13)$$

and the dark states ρ must have a block-diagonal form:

$$\rho = \sum_{\{s;d_s>1\}} P_s \rho P_s = \sum_{\{s;d_s>1\}} p_s \rho_s, \quad (14)$$

where $\rho_s = P_s \rho P_s / \text{Tr}[P_s \rho P_s]$ is a $d_s \times d_s$ normalized density matrix, and $p_s = \text{Tr}[P_s \rho P_s]$.

The second constraint given by Eq. (10) can now be written as

$$\forall s; \quad d_s > 1 \quad QHP_s \rho_s = 0. \quad (15)$$

We deduce that ρ_s can in principle be any positive, Hermitian, with trace-one linear operator defined on $\ker[QHP_s]$, the kernel of $QHP_s \subset P_s \mathcal{H}$.

To conclude this section, we summarize: To have a dark state, PHP must have a degenerate spectrum; this puts a constraint on the laser frequencies. The dark state is a statistical superposition of states ρ_s , defined on $\ker[QHP_s]$, where P_s are the orthogonal projectors on the eigensubspaces of PHP , corresponding to degenerate eigenvalues of PHP . Depending on the dimension of $\ker[QHP_s]$ this last condition may or may not impose a condition on the Rabi frequencies V_{ij} ; this is the subject of the next section.

Notice that including dissipation or dephasing within the ground-state manifold destroys the interference of the transition amplitudes to the excited states, and it leads the system to a bright state where it partially populates the excited states. These scenarios have been considered in previous work where the fluorescence intensity has been proposed as a measure of the ground-state decoherence rate [44].

C. Dimension, unicity, and purity

In addition to the constraint on laser frequencies, the condition that ρ_s must be defined on $\ker[QHP_s]$ can be satisfied if and only if the $\ker[QHP_s]$ is not empty, $\dim[\ker[QHP_s]] \geq 1$. By the rank-nullity theorem, $\dim[\ker[QHP_s]] + \text{rank}[QHP_s] = \text{rank}[P_s] = d_s$. Hence, a dark state can exist if and only if for at least one of the eigensubspace $P_s\mathcal{H}$ of dimension d_s ,

$$\text{rank}[QHP_s] \leq d_s - 1. \quad (16)$$

As $\text{rank}[QHP_s] \leq \text{rank}[Q] = N_e$, then two different cases are in order:

Case 1. $N_e \leq d_s - 1$. In this case, Eq. (16) is always fulfilled, regardless of the values taken by the Rabi frequencies V_{ij} . The constraint on the laser frequencies ω_{ij} , giving the degeneracy of PHP and determining the dimension d_s of the eigensubspace is necessary and sufficient for the existence of a dark state. We have supposed that the constraint imposed by the RWA [Eq. (6)] has already been fulfilled. The Λ , the M systems, and the so-called fan [34] or multipod systems [28] belong to this case. They are discussed in more detail in the next section.

Case 2. $N_e \geq d_s$. In this case, $\text{rank}[QHP_s] \leq N_e - 1 < N_e = \text{rank}[Q]$. Lowering the rank of QHP_s to a lower value than $\text{rank}[Q]$ cannot be obtained for all values of the Rabi frequencies. In other words, the V_{ij} must satisfy some relations such that the kernel QHP_s be nonempty. Therefore, in this case, the existence of a dark state requires that, in addition to the laser frequencies ω_{ij} , the Rabi frequencies V_{ij} must fulfill some constraints. The specific case $N_g = N_e = 2$ which belongs to this case is discussed in more detail in the next section.

In general, we see that when $\dim[\ker[QHP_s]] > 1$, or when there is more than one eigenvalue of PHP which is degenerate, then multiple dark states may exist. More specifically, the stationary dark state can be represented by any density operator ρ defined on $\bigoplus_{\{s; d_s > 1\}} \ker[QHP_s]$ [see Eqs. (14) and (15)]. That is, if $N_s = \dim[\ker[QHP_s]]$, then a stationary dark state can be represented by any block-diagonal $M \times M$ density matrix, where $M = \sum_{\{s; d_s > 1\}} N_s$, where the sum runs over all degenerate eigensubspaces $P_s\mathcal{H}$ of H , and each block is an $N_s \times N_s$ positive, Hermitian matrix. Therefore, the stationary dark state which is reached asymptotically in time will depend on the initial state. The dark state will be unique if and only if there is only one eigenvalue \mathcal{E}_s which is degenerate, and $\dim[\ker[QHP_s]] = 1$. We note that in this case the dark state is a pure state. We conclude that, for dark states, unicity implies purity. Hence, if there is a mixed dark state then it is not unique. Indeed, suppose that the dark state is a mixed state $\rho = p_1|\psi_1\rangle\langle\psi_1| + p_2|\psi_2\rangle\langle\psi_2|$, where p_1 and p_2 are the eigenvalues of ρ and $|\psi_1\rangle$, $|\psi_2\rangle$, are the two corresponding

orthonormal eigenvectors. Because ρ is a dark state, its two eigenstates must belong to $\ker[PHP]$. But then any linear combination or any statistical superposition of two states will fulfill the dark-state condition in Eq. (10). Then, there is not a unique dark state.

A simple way to achieve a unique dark state is to tune the frequencies such that the dimension of the unique degenerate subspace d_s fulfills the equality $N_e = d_s - 1$. As we are in case 1 ($N_e \leq d_s - 1$), there is a dark state regardless of the values of the V_{ij} , but in addition, $\dim[\ker[QHP_s]] = d_s - \text{rank}[PHQ] = d_s - N_e = 1$. In this case, $\text{rank}[PHQ] = N_e = d_s - 1$ because we suppose that each considered excited state $|e_j\rangle$ is coupled to at least one ground state $|g_i\rangle$ by a Rabi frequency V_{ij} .

This is why such M systems [34] have attracted attention as a generalization of the very well-known Λ systems where $d_s = N_g = 2$ and $N_e = 1$. Specific examples illustrating these general considerations are given in the next section.

III. EXAMPLES

In this section we illustrate the preceding discussion with four examples that show the different cases from Sec. II C: a case with a unique stationary dark state, a case with a dark stationary subspace, and a case that is overspecified and whose dark state depends on the Rabi frequencies. The fourth example is the more complex system of the 11 hyperfine levels of ^{87}Rb . For each case, we review the necessary condition to have a degenerate subspace and a nonzero kernel for QHP , and the resulting dark-state subspaces. We numerically calculate the time evolution of the density matrix by evolving a single initially populated ground level with the Lindbladian of the system $\rho(t) = e^{L t} \rho(0)$.

A. Example 1: Unique stationary state for zigzag systems

$$(N_g = N_e + 1)$$

We refer to zigzag or M systems as those where the connectivity given by the laser fields follows the pattern ground-(excited-ground) $_n$ [Fig. 2(a)]. We consider in particular the M system with $N_g = 3$ and $N_e = 2$ which has been discussed elsewhere [29]. It is a system where $N_g = N_e + 1$ so that $\dim[\ker[QHP]] = 1$ and $\dim[\ker[L]] = 1$, provided that all detunings are equal. Figure 2(a) shows the evolution of the populations with initial conditions $\rho(t=0) = |e_1\rangle\langle e_1|$ in the site basis $\{|g_i\rangle; i = 1, 2, 3\}$, $\{|e_j\rangle; j = 1, 2\}$ and in the eigenstate of the H basis $\{|\phi_n\rangle; n = 1, \dots, 5\}$. As expected, the system evolves towards a pure dark state, which here is $|\phi_5\rangle$.

Variations on the zigzag systems can be obtained by introducing additional coupling between ground and excited states. These modify the configuration of the stationary state over the ground-state sites but do not change its existence, uniqueness, or purity. Because these additional couplings create connectivity loops, the frequency of these additional laser fields cannot be independently chosen if we want to satisfy the RWA [Fig. 2(b) and Appendix A]. In the particular case we are considering [see Fig. 2(b)], the additional Rabi frequency V_{31} must correspond to a laser frequency ω_{31} fulfilling $\omega_{31} = \omega_{21} + \omega_{32} - \omega_{22}$. The maximum number of couplings is $N_g N_e$,

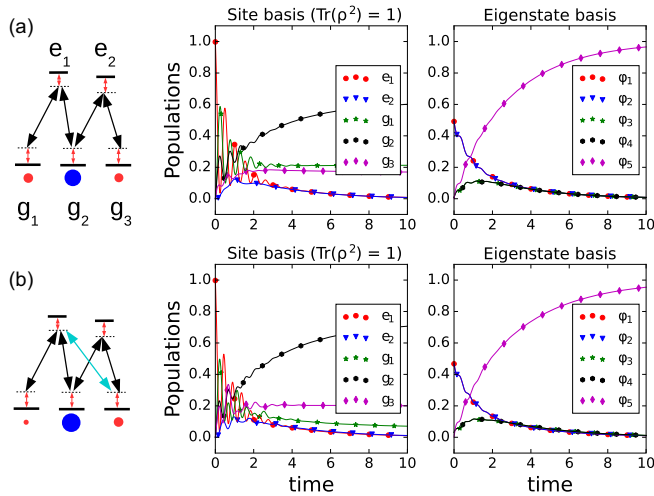


FIG. 2. Populations of the M system as a function of time in the (a) diagram of the M system connectivity and probability amplitudes of the pure, dark, stationary state (red is positive probability amplitude, blue is negative). The dynamics of the system is plotted in the site basis and in the eigenstate basis. The system evolves towards a pure state occupying only the ground states. Parameters are $V_{21} = 0.56$, $V_{22} = 0.23$, $V_{32} = 0.45$, $\gamma_{11} = 0.04$, $\gamma_{12} = 0.01$, $\gamma_{13} = 0.09$, $\gamma_{21} = 0.14$, $\gamma_{22} = 0.02$, and $\gamma_{23} = 0.04$. (b) Same as in (a) in the presence of the coupling $V_{31} = 0.57$. In both cases the dark state is ϕ_5 (all values in units of V_{11}).

one for each couple (g_i, e_j) . Other control fields that fall beyond the scope of this article are worth mentioning. For example, Cerrillo *et al.* [39–42] proposed the addition of a control field between the ground states of a Λ system as a means for accelerating the cooling rate. While the ground state can be prediagonalized and the magnitude of the ground-excited couplings redefined (thus leading to the starting point of this article), this has as a consequence to mix the restriction on detunings with restrictions on Rabi frequencies, resulting in dark states that depend on the intensity of the laser field as well. This point is retaken in example 3, where other examples of intensity-dependent dark states are illustrated.

B. Example 2: Dark stationary subspace for fan systems

$$(N_g \geq 2, N_e = 1)$$

Fan or multipod systems consist of N_g ground states and a single excited state (the Λ configuration is also an instance of a fan system although it has a unique stationary state). In general the stationary states of fan systems can be arranged in a number of degenerate subspaces, generated by pure states $|\phi_n\rangle = \sum_{i=1}^{d_s} c_{ni}|g_i\rangle$ where from Eq. (10), the coefficients c_{ni} must fulfill

$$\sum_{i=1}^{d_s} V_{i1} c_{ni} = 0, \quad (17)$$

where V_{i1} are the Rabi frequencies of the laser coupling ground state $|g_i\rangle$ and the unique excited state $|e_1\rangle$. Fan systems have stationary states of high multiplicity: for each subspace of dimension d_s the kernel of the Liouvillian will have a

dimension $(d_s - 1)^2$ as well as $(d_s - 1)^2$ conserved quantities (obtained as the left eigenvalues of the Liouvillian [36,45]).

We specifically consider the case $N_g = 4$. We begin with all four ground states forming a degenerate manifold and detune them one by one to assess its effect on the steady state—whether it remains dark, pure, and how its multiplicity changes. We choose equal couplings to the excited state for ease of visualization, and unequal relaxations back to the ground state ($V_{11} = V_{21} = V_{31} = V_{41} = 1$, and $\gamma_{11} = 0.1$, $\gamma_{12} = 0.2$, $\gamma_{13} = 0.3$, $\gamma_{14} = 0.4$).

a. Fully degenerate ($d_1 = 4$). The fully degenerate fourfold ground-state case has $\dim[\ker[QHP]] = 3$ and $\dim[\ker[L]] = 9$ [Fig. 3(a)]. A system initially in the excited state will evolve towards a mixed 3×3 density matrix ($\text{Tr}(\rho^2) = 0.38$) determined by the conserved quantities that depend on the relaxation rates. Thus, although the condition to have the dark states depends exclusively on the Rabi frequencies and frequency detunings, the steady-state density matrix also depends on the relaxation rates and on the initial state.

b. One detuned ground state ($d_1 = 3$). The system qualitatively similar to case (a) has $\dim[\ker[QHP]] = 2$ and $\dim[\ker[L]] = 4$ [Fig. 3(b)]. The evolution converges towards a 2×2 density matrix corresponding to a mixed state ($\text{Tr}(\rho^2) = 0.51$).

c. Pairwise degenerate states ($d_1 = 2$ and $d_2 = 2$). Detuning a second ground state to the same value as the one of case (b) results in pairwise degenerate levels [Fig. 3(c)]. We must separately consider the degenerate subspaces, so we have $\dim[\ker[QHP_1]] = 1$ and $\dim[\ker[QHP_2]] = 1$, and $\dim(\ker(L)) = 1^2 + 1^2 = 2$. The evolution converges to the mixture of two pure states $p_1|\phi_1\rangle\langle\phi_1| + p_2|\phi_2\rangle\langle\phi_2|$, where each $|\phi_n\rangle$ ($n = 1, 2$) is the stationary state of a Λ system. The weights p_n ($n = 1, 2$) depend on the dissipation rates. These are larger for the second manifold ($|g_3\rangle, |g_4\rangle$) than for the first one ($|g_1\rangle, |g_2\rangle$) and so the second manifold is more heavily populated.

d. Minimum degenerate manifold ($d_1 = 2$). The final detuning scheme keeps only a degenerate pair of levels [Fig. 3(d)]. Then, $\dim(\ker(QHP_1)) = 1$ and $\dim(\ker(L)) = 1$. Because the dark state is unique, it is also pure (as shown in Sec. II C). By properly choosing the detunings an experimentalist can localize in energy or space (if each energy level is spatially separated) via pumping.

We also note that because the excited states relax to the ground state, any dark state will accumulate all population and become the steady state of the system. This is why in case (d) the detuning of the other ground states does not render the state bright.

C. Example 3: A Rabi frequency conditioned dark state: Pairs of two-level systems ($N_g \leq N_e$)

We consider a system with two levels in the excited state and two levels in the ground state (Fig. 4). As $d_s = 2$, we have $\dim[\ker[QHP]] = 2 - \text{rank}[QHP]$. The generic case corresponds to $\text{rank}[QHP] = \text{rank}[Q] = 2$ and in this case the kernel is empty—no dark state can exist in general, in contrast to the previous two examples. We see that a dark state may exist but not for all values of the Rabi frequencies V_{ij} . Furthermore, the existence of a loop in the connectivity constrains the laser

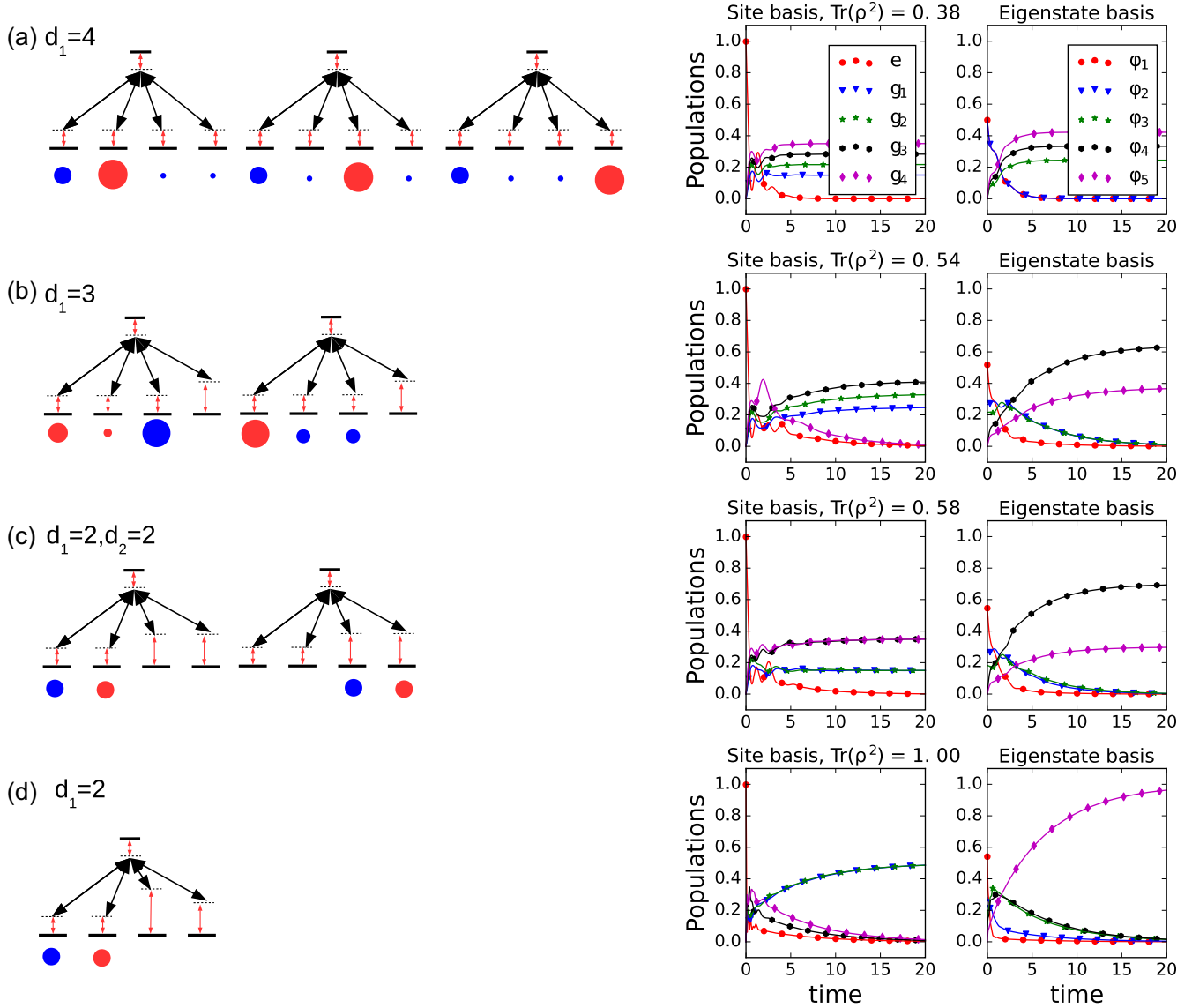


FIG. 3. Tripod system with four ground-state levels in different detuning configurations. Below the systems are shown the wave functions that span the dark-state subspace (blue means negative coefficient, red positive coefficient, and the size of the circle is proportional to the coefficient). On the left side are shown the evolution of the populations for an initially excited state. The purity of the steady state is evaluated by calculating $\text{Tr}(\rho_{SS}^2)$. Parameters of the simulations are $V_{21} = V_{31} = V_{41} = 1$, and $\gamma_{11} = 0.1$, $\gamma_{12} = 0.2$, $\gamma_{13} = 0.3$, $\gamma_{14} = 0.4$ (all values in units of V_{11}).

frequencies to fulfill the relation $\omega_{21} = \omega_{11} + \omega_{22} - \omega_{12}$, such that the RWA results in a time independent Hamiltonian (see Appendix A).

The Hamiltonian is (after a convenient referencing of the zero point energy)

$$H = \begin{bmatrix} 0 & 0 & V_{11} & V_{12} \\ 0 & \mathcal{E}_2 & V_{21} & V_{22} \\ V_{11}^* & V_{21}^* & \mathcal{E}_3 & 0 \\ V_{12}^* & V_{22}^* & 0 & \mathcal{E}_4 \end{bmatrix}. \quad (18)$$

The degeneracy condition implied by Eq. (9) requires that $\mathcal{E}_2 = 0$. The constraint given by Eq. (15) results in a relation between Rabi frequencies:

$$V_{11}V_{22} = V_{12}V_{21}. \quad (19)$$

Figures 5(a) and 5(b) show the dynamics for a Λ system and an $N_g = 2, N_e = 2$ system, respectively, to compare the effect of an additional excited state tuned to the dark-state condition. Although the dynamical evolution differs slightly, the stationary state is identical. Increasing one of the Rabi frequencies gets the system out of the dark-state condition onto a mixed stationary state where all four states are occupied, as shown in Fig. 5(c).

We can understand the setup and restrictions on the Rabi frequencies by viewing the system as a pair of Λ geometries on the same ground states. Because only one excited level is enough to fully specify the dark-state condition (in general to fully specify a unique dark state in an N_g degenerate state one needs at least $N_g - 1$ excited states), the second Λ system must be adapted to the ground-state population specified by

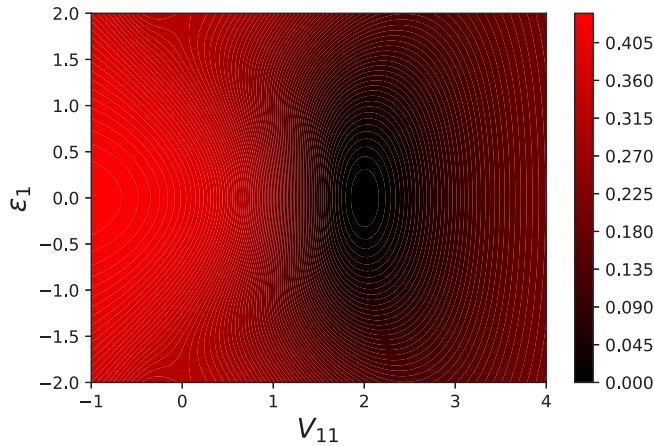


FIG. 4. Excited-state population as a function of detuning and field intensities for a pair of two-level systems. Parameters of the simulations are $V_{12} = 2$, $V_{11} = 1$, and $\gamma_{11} = 0.2$, $\gamma_{12} = 0.5$, $\gamma_{21} = 0.44$, $\gamma_{22} = 0.7$ (all values in units of V_{22}).

the first Λ system. This involves not only the intensities but also the phases of the fields. It is important to remark that it is not the photons of the field but the transition amplitudes which interfere destructively (or not), and which depend on the phase of the wave function in the ground state. The first pair of fields (acting on the same excited state) determines all the coefficients of the ground state. For the transition

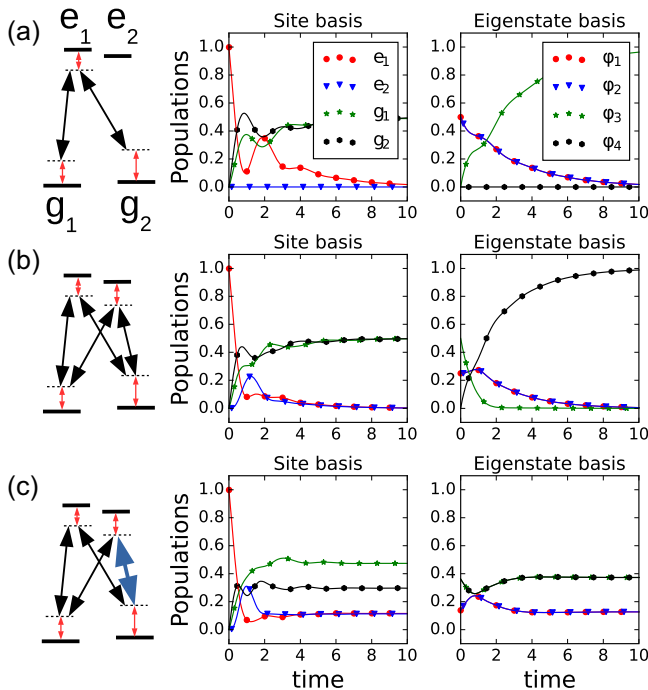


FIG. 5. Excited-state population for a pair of two-level systems in the case of (a) only coupling to one excited state ($V_{21} = 1$), (b) coupling to both excited states in the dark-state condition ($V_{21} = 1$, $V_{12} = 1$, and $V_{22} = 1$), and (c) coupling to both excited states not fulfilling the dark-state condition ($V_{21} = 1$, $V_{12} = 1$, and $V_{22} = 2$). The relaxation rates are $\gamma_{11} = 0.2$, $\gamma_{12} = 0.5$, $\gamma_{21} = 0.44$, $\gamma_{22} = 0.7$ (all values in units of V_{11}) and all detunings have been set equal.

dipole amplitudes of the second pair of pulses to interfere destructively, these must have both the correct intensity and phase. Not doing so imposes a second set of conditions on the phase and amplitude of the wave-function coefficients which does not result in the destructive interference of the transition amplitudes induced by the first pair of fields.

The map of excited-state population vs Rabi frequency and detuning (see Fig. 4) reveals a dark state in frequency detuning as well as in Rabi frequency. The asymmetry in the map between positive and negative values of the Rabi frequency illustrates the phase sensitivity of the dark state.

Given a complex coupling $V_{ij} = F_{ij}e^{i\phi_{ij}}$, the requirement (19) separates into a constraint on the magnitudes of the fields $|F_{11}||F_{22}| = |F_{12}||F_{21}|$ and on the relative phases $\phi_{11} + \phi_{22} = \phi_{12} + \phi_{21}$. Such a dependence of the dark state on the Rabi frequencies could result in new metrology tools. Such phase-sensitive dark states were initially investigated theoretically in a double- Λ system [46] and experimentally [47]. They are currently one of the newest research avenues [48] due to their possibility of shifting the laser phase without a cavity [49].

D. Hyperfine splittings of ^{87}Rb atoms

The characteristics of dark states outlined here allow a shortcut to establish their presence in more complex systems. As an example we take the study of CPT in multi-Zeeman-sublevel ^{87}Rb atoms, as considered by Ling *et al.* [50]. In their publication, Ling *et al.* investigated the possibility of obtaining CPT using only two copropagating linearly polarized lasers addressing the two transitions that connect the higher energy level $P_{1/2}$, $F' = 1$ to the two lower levels $S_{1/2}$, $F = 2$ and $S_{1/2}$, $F = 1$, respectively. The main point is that each of these three levels has a hyperfine sublevel structure. Indeed, the $S_{1/2}$, $F = 2$ is composed by five degenerated sublevels ($m_F = -2, -1, \dots, 2$), and both $P_{1/2}$, $F' = 1$ and $S_{1/2}$, $F = 1$ are composed by three degenerated sublevels each ($m_F = -1, 0, 1$). Taking the quantization axis as the propagation direction results in σ^+ , σ^- transitions with equal strength, as both lasers are linearly polarized [50]. The energy levels as well as all possible transitions (σ^+ , σ^- , and s) are shown in Fig. 6 (boxed scheme).

We expand the scope of possible transitions beyond those considered by Ling *et al.* by introducing additional lasers that can induce $\Delta m_F = 0$ and $\Delta m_F = \pm 1$ transitions. The selected schemes are shown in Fig. 6. We apply to these cases the criteria developed in this article to obtain the number, dimension, and purity of dark states without the need for expensive numerical simulations.

As a first step we identify the number of degenerate subspaces that can independently sustain dark states [see Eq. (13)]. These degenerate subspaces can occur on account of different detunings (see, e.g., Fig. 3), or because the connectivity results in two decoupled (ground-excited) systems such as in schemes 1, 3, 6, and 7 of Fig. 6. For simplicity we assume in our analysis that all detunings are equal. The next step is to calculate the kernel of QHP_s [see Eq. (15)]. The dimension of the resulting dark-state manifold is $\dim[\ker(QHP_s)] = d_s - \dim[\text{rank}(QHP_s)]$. For the connectivities considered, if $N_g > N_e + 1$, there will always be a dark state for any field intensity, provided that the detuning condition is met (we

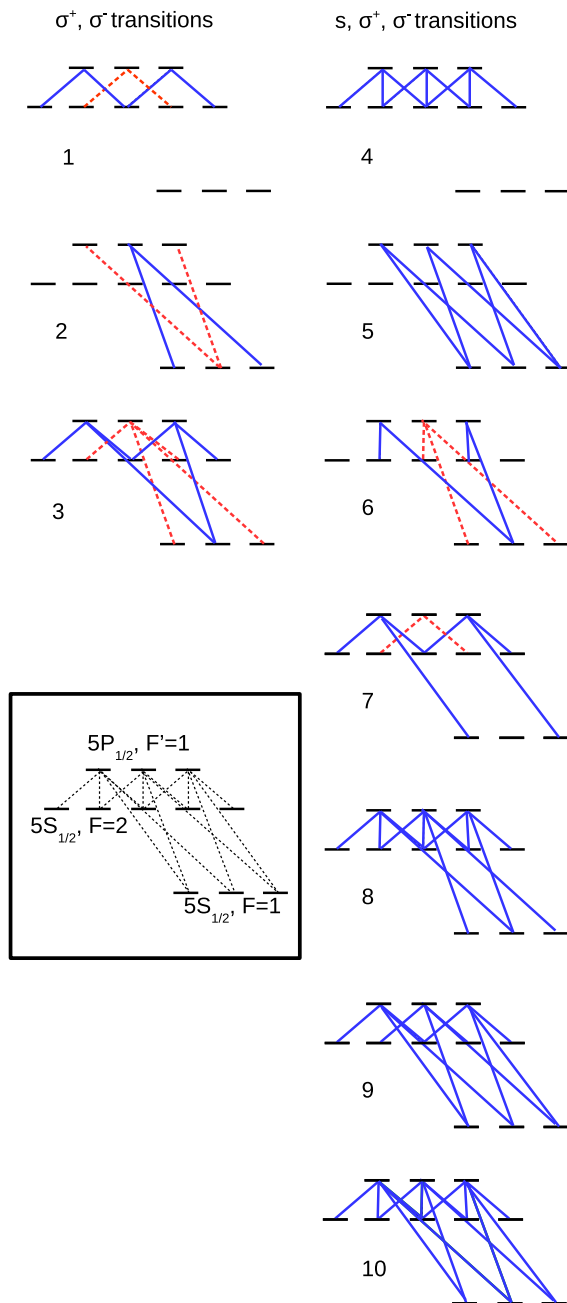


FIG. 6. Possible connectivities for the hyperfine levels of ^{87}Rb atoms. In the case of multiple manifold of dark states these are labeled by different colors (blue (solid) corresponds to d_1 and red (dashed) corresponds to d_2 of Table I). The case investigated in Ref. [50] corresponds to case 3.

note that N_g and N_e are only defined with respect to coupled states so that, for instance, $N_g = 5$ in scheme 1 of Fig. 6 and the sublevels of the $F = 1$ manifold do not contribute to N_g). These are the cases of all schemes except scheme 5. In this case, we need that $\dim[\text{rank}(QHP_s)] < N_e$, which can be obtained in the case by adjusting the intensities. The conditions are $-V_{11}V_{23}V_{32} = V_{12}V_{21}V_{33}$, where we have used the nomenclature of this paper where the first index labels a ground state and the second an excited state. In the specific

case of the hyperfine transitions of ^{87}Rb this transforms into $-V_sV_{\sigma^+}V_{\sigma^-} = V_{\sigma^+}V_{\sigma^-}V_s$, which has no solution given that different $\Delta m_F = \pm 1$ transitions cannot be independently controlled (this might be different for other physical systems of three ground-excited pairs). We gather in Table I our results. The existence of a dark state, its dimension, and its purity are indicated, as well as the levels spanned by the state. From this table more involved calculations such as have been carried out for Λ systems can more seamlessly be extended [51–54].

Having such a summary can be of further use since one can imagine preparing a pure dark state in the red (dashed) subsystem of scheme 1 (population in levels $F = 2, m_F = -1, +1$) by first preparing the dark state of scheme 2 ($F = 1, m_F = -1, +1$), and adiabatically turning on the $F' = 1$ to $F = 2$ transition to transfer populations adiabatically to the $F = 1, M = -1, +1$ levels, and turning off the laser for the $F = 1$ to $F' = 1$ transition to result in a pure state of scheme 1 ($F = 2, M = -1, +1$), without any population in the $F = 2, M = -2, 0, +2$ dark state. Such a state is not obvious to prepare, but becomes more transparent from our analysis. We remark that for several of these cases nonidealities play different roles. Collisional relaxation among the ground-state manifold induces a small population in the excited states. We also remark that in the cases where certain states are uncoupled by light but coupled by dissipative pathways (cases 1 and 4–7), some of the population might be lost to them (i.e., sink states).

IV. CONCLUSIONS

We have presented an overview of dark-state conditions on dissipative systems classified as a function of the number of ground and excited states. The condition can be reduced to a condition on the Hamiltonian part of the evolution. The number of excited and ground states naturally separates the systems into a case where CPT depends only on the detunings, and one where CPT appears only when conditions on the detunings, the Rabi frequencies, and their phases are met. When the kernel has multiplicities higher than one, the stationary states are mixed and the term “coherent population trapping” becomes less apt. Conserved quantities determine the final state and these depend on the dissipative rates of the system.

ACKNOWLEDGMENTS

D.F.S. acknowledges support from the European Union through the Marie Skłodowska-Curie Grant Agreement No. 702694. S.F. acknowledges support from the PRESTIGE program, under the Marie Curie Actions-COFUND of the FP7.

APPENDIX A: ROTATING WAVE APPROXIMATION

We use throughout the article the RWA to turn the time-dependent Hamiltonian into a time-independent Hamiltonian. For N -level systems with arbitrary connectivity this may impose important constraints on the wavelengths or detunings that can be used.

Let us start from the original time-dependent Schrödinger equation for the unitary evolution operator generated by the

TABLE I. Characteristics of the dark states corresponding to the systems illustrated in Fig. 6. The first three columns indicate the polarization of the laser inducing the $F = 2 \leftrightarrow F' = 1$ transition and the next three columns are for the laser polarization coupling the states corresponding to the $F = 1 \leftrightarrow F' = 1$ transition. In some case two manifolds of dark states can take place: columns d_1 and d_2 . In each d_1 and d_2 column, the atomic states involved, the dimension, the purity, and the number of cycles of the dark states are indicated. Scheme 5 is marked as a dark state, although the conditions imposed on the intensities cannot be fulfilled with the radiative transitions' degrees of freedom considered here (see text for details).

	d_1 States			Dimension Purity Cycles			d_2 States			Dimension Purity Cycles					
	s	σ^+	σ^-	F	M		Dimension	Purity	Cycles	F	M		Dimension	Purity	Cycles
1	x	x		$F = 2, M = -2, 0, +2$			1	yes	0	$F = 2, M = -1, +1$			1	yes	0
2		x	x	$F = 1, M = -1, +1$			1	yes	0						
3	x	x	x	$F = 2, M = -2, 0, +2/F = 1, M = 0$			2	no	1	$F = 2, M = -1, +1/F = 1, M = -1, +1$			3	no	0
4	x	x	x	$F = 2, M = -2, -1, 0, +1, +2$			2	no	2						
5		x	x	$F = 1, M = -1, 0, +1$			1	yes	1						
6	x		x	$F = 2, M = -1, +1/F = 1, M = 0$			1	yes	0	$F = 2, M = 0/F = 1, M = -1, +1$			2	no	0
7	x	x	x	$F = 2, M = -2, 0, +2/F = 1, M = -1, +1$			3	no	0	$F = 2, M = -1, +1$			1	yes	0
8	x	x	x	$F = 2, M = -2, -1, 0, +1, +2/F = 1, M = -1, 0, +1$			5	no	3						
9	x	x	x	$F = 2, M = -2, -1, 0, +1, +2/F = 1, M = -1, 0, +1$			5	no	2						
10	x	x	x	$F = 2, M = -2, -1, 0, +1, +2/F = 1, M = -1, 0, +1$			5	no	5						

time-dependent Hamiltonian $H(t)$, $i\dot{U}(t) = H(t)U(t)$, where $H(t)$ can be written as

$$H(t) = \sum_{i=1}^N E_i |i\rangle\langle i| + \sum_{i>j=1}^N F_{ij}(t)(|i\rangle\langle j| + |j\rangle\langle i|) \quad (\text{A1})$$

and $F_{ij}(t) = 2F_{ij} \cos(\omega_{ij}t + \phi_{ij})$, where the F_{ij} , ω_{ij} and ϕ_{ij} are time-independent constants.

We look for a diagonal operator $H_0 = \sum_{i=1}^N \epsilon_i |i\rangle\langle i|$, such that after applying the unitary operator $U_0 = e^{-iH_0 t}$, the original time-dependent Schrödinger equation becomes time independent within a good approximation.

Specifically, let us write $U(t) = U_0(t)U_I(t)$; then $U_I(t)$ fulfills the Schrödinger $i\dot{U}_I = H_I(t)U_I(t)$, where $H_I = \sum_{i=1}^N (E_i - \epsilon_i)|i\rangle\langle i| + V(t)$ and $V(t)$ is given by

$$V(t) = \sum_{i>j=1}^N F_{ij}(t)(e^{i(\epsilon_i - \epsilon_j)t} |i\rangle\langle j| + \text{H.c.}), \quad (\text{A2})$$

where H.c. means the Hermitian conjugate of the preceding term.

Using the explicit expression of $F_{ij}(t)$ as $F_{ij}(t) = (V_{ij}e^{i\omega_{ij}t} + V_{ij}^*e^{-i\omega_{ij}t})$, where $V_{ij} = F_{ij}e^{i\phi_{ij}}$, we obtain

$$V(t) = \sum_{i>j=1}^N (V_{ij}e^{i(\epsilon_i - \epsilon_j - \omega_{ij})t} |i\rangle\langle j| + \text{H.c.}) + (V_{ij}e^{i(\epsilon_i - \epsilon_j + \omega_{ij})t} |i\rangle\langle j| + \text{H.c.}) \quad (\text{A3})$$

The RWA consists in choosing a set of energies ϵ_i such that

$$\epsilon_i - \epsilon_j = \omega_{ij} \quad (\text{A4})$$

and such that the terms oscillating at the frequencies $\epsilon_i - \epsilon_j + \omega_{ij} = 2\omega_{ij}$, corresponding to the third line of Eq. (A3), can be safely neglected.

Within this approximation, $U_I(t)$ fulfills a time-independent Schrödinger equation, $U_I \simeq H_I U_I(t)$, where H_I is time independent and given by

$$H_I = \sum_{i=1}^N (E_i - \epsilon_i)|i\rangle\langle i| + \sum_{i>j=1}^N (V_{ij}|i\rangle\langle j| + \text{H.c.}). \quad (\text{A5})$$

It is convenient to introduce the operators $\sigma_{ij}^z = |i\rangle\langle i| - |j\rangle\langle j|$ and take advantage of the condition Eq. (A4), in order to rewrite H_I as

$$H_I = \sum_{i>j=1}^N [\Delta_{ij}\sigma_{ij}^z + (V_{ij}|i\rangle\langle j| + \text{H.c.})], \quad (\text{A6})$$

where we have defined the detunings $\Delta_{ij} = E_i - E_j - \omega_{ij}$ and where we have ignored a term proportional to the identity which corresponds to an arbitrary energy origin.

The unitary transform U_0 does not affect the dissipative part of the Lindblad operator [Eq. (2)]. Indeed, $\rho_I = U_0^\dagger \rho U_0$ fulfills the Lindblad equation $\dot{\rho}_I = -i[H_I, \rho_I] + \sum_{\{ij\}} \gamma_{ij} D_{ij}(\rho)$ as $U_0^\dagger D_{ij}(\rho) U_0 = D_{ij}(\rho)$ [see Eq. (5)]. Therefore, within the RWA, the Lindblad operator is time independent.

We note that this is possible only if we can find a solution of Eq. (A4), giving the N unknowns ϵ_i , as a function of the

laser frequencies ω_{ij} . We infer that in general the number of equation must be less than N . But this constraint is not sufficient. Even when the number of equations is less than N , additional constraints on the laser frequencies ω_{ij} may be imposed to obtain a solution of Eq. (A4). This is always the case when there is a closed cycle in the set of couple (i, j) . For example, consider an N -level system with $N \geq 3$, where the transitions $(i, j) = (1, 2), (2, 3)$, and $(1, 3)$ are driven by three different laser fields. Then, summing Eq. (A4), over i and j , with $i > j$, gives $\omega_{12} + \omega_{23} + \omega_{13} = 0$.

APPENDIX B: PROOF OF THEOREM 1

Proof. If $\det[L_{\tilde{H}}] = 0$, then $L_{\tilde{H}}$ has a right eigenvector ρ_d which fulfills $\tilde{H}\rho_d - \rho_d\tilde{H}^\dagger = 0$. ρ_d is a steady state of the dynamics generated by $L_{\tilde{H}}$. We separate explicitly the Hermitian and non-Hermitian parts of \tilde{H} and this condition becomes

$$[H, \rho_d] - i\{\Gamma, \rho_d\} = 0, \quad (\text{B1})$$

where Γ is given by $\Gamma = \sum_{(ij)} \gamma_{ij}(\sigma_{ij}^\dagger \sigma_{ij})$ with $\sigma_{ij} = |g_i\rangle\langle e_j|$ or

$$\Gamma = \sum_{j=1}^{N_e} \Gamma_j |e_j\rangle\langle e_j| \quad (\text{B2})$$

with $\Gamma_j = \sum_{i=1}^M \gamma_{ij} > 0$ is the total decay rate of the excited state $|j\rangle$. Hence, Γ is a completely positive diagonal matrix and the ground-state manifold $\{|g_i\rangle\}$ is a subspace of its kernel, $\Gamma|g_i\rangle = 0; \forall i = 1, 2, \dots, M$.

Taking the trace of Eq. (B1) gives us $\text{Tr}[\Gamma\rho_d] = 0$, as the trace of the commutator gives zeros. Using Eq. (B2), this last condition can be written as

$$\sum_{j=1}^{N_e} \Gamma_j \langle e_j | \rho_d | e_j \rangle = 0. \quad (\text{B3})$$

But each term of this sum is positive; therefore, each term must be zero, thus $\langle e_j | \rho_d | e_j \rangle = 0; \forall j = 1, 2, \dots, N_e$. We conclude that ρ_d has no population in the excited-state manifold; therefore, it cannot have coherence involving excited states, $\langle e_j | \rho_d | e_{j'} \rangle = \langle e_j | \rho_d | g_i \rangle = 0$. We conclude that ρ_d lies in the ground-state manifold $\{|g_i\rangle\}$.

Now we consider the original Lindblad operator L which includes the quantum jump operator $\sum_{ij} \gamma_{ij} \sigma_{ij} \rho_d \sigma_{ij}^\dagger$, written explicitly as

$$J(\rho_d) = \sum_{ij} |g_i\rangle\langle e_j | \rho_d | e_j \rangle \langle g_i| = 0, \quad (\text{B4})$$

where we have used $\langle e_j | \rho_d | e_j \rangle = 0$. Therefore, $L\rho_d = 0$.

Finally ρ_d is a steady state of L with no component in the excited-state manifold, hence it is a dark state. ■

We have thus proved that if $L_{\tilde{H}}\rho = 0$ then ρ is a dark state. The converse is obviously true.

APPENDIX C: FROM SUPERPROJECTOR TO PROJECTOR

Starting from the equations

$$\begin{aligned} \mathcal{P}L_{\tilde{H}}\mathcal{P}\rho + \mathcal{P}L_{\tilde{H}}\mathcal{Q}\rho &= 0, \\ \mathcal{Q}L_{\tilde{H}}\mathcal{P}\rho + \mathcal{Q}L_{\tilde{H}}\mathcal{Q}\rho &= 0, \end{aligned} \quad (\text{C1})$$

we would like to prove their equivalence with the following equations:

$$[PHP, \rho] = 0, \quad (\text{C2})$$

$$QHP\rho = 0. \quad (\text{C3})$$

We first enforce $\rho = \mathcal{P}\rho$ and $\mathcal{Q}\rho = 0$. Then

$$\mathcal{P}L_{\tilde{H}}\mathcal{P}\rho = 0, \quad \mathcal{Q}L_{\tilde{H}}\mathcal{P}\rho = 0. \quad (\text{C4})$$

It is convenient to introduce the column form ρ_s of ρ , which converts an $n \times n$ matrix ρ to an n^2 column vector ρ_s . In this transformation, the operation $A\rho B^\dagger$ is mapped to $\tilde{B} \otimes A\rho_s$, where \tilde{B} denotes the conjugate of B [55].

The effect of this mapping on the superprojector is as follows:

$$\begin{aligned} \mathcal{P}\rho &\rightarrow P \otimes P\rho_s, \\ \mathcal{Q}\rho &\rightarrow (P \otimes Q + Q \otimes P + Q \otimes Q)\rho_s. \end{aligned} \quad (\text{C5})$$

The superoperator $L_{\tilde{H}}$ is mapped as

$$L_{\tilde{H}}\rho \rightarrow -i(\mathbb{1} \otimes \tilde{H} - \tilde{H}^t \otimes \mathbb{1})\rho_s, \quad (\text{C6})$$

where \tilde{H}^t is the transpose of \tilde{H} . Using Eqs. (C5) and (C6), we can map Eqs. (C4) as

$$(P \otimes PHP - PHP \otimes P)\rho_s = 0, \quad (\text{C7})$$

$$(P \otimes QHP - Q\tilde{H}^t P \otimes P)\rho_s = 0, \quad (\text{C8})$$

where we have used that $P\tilde{H}P = P\tilde{H}^t P = PHP$ and $Q\tilde{H}P = QHP$. By reversing the mapping, the first equation [Eq. (C7)] gives

$$[PHP, P\rho P] = 0, \quad (\text{C9})$$

which is Eq. (9) of the main text.

For the second equation [Eq. (C8)], we use that the dark state fulfills $\rho = P\rho P$. Therefore, the second term $Q\tilde{H}^t P \otimes P\rho_s = 0$. Indeed, by reversing the mapping, it can be written as $P\rho P Q\tilde{H}^\dagger P = 0$. Hence, Eq. (C8) is equivalent to $P \otimes QHP\rho_s = 0$, which, by reversing the mapping, gives

$$QHPP\rho P = 0, \quad (\text{C10})$$

which is Eq. (10) of the main text.

- [1] P. M. Radmore and P. L. Knight, *J. Phys. B* **15**, 561 (1982).
 [2] K. Bergmann, H. Theuer, and B. W. Shore, *Rev. Mod. Phys.* **70**, 1003 (1998).

- [3] K.-J. Boller, A. Imamoglu, and S. E. Harris, *Phys. Rev. Lett.* **66**, 2593 (1991).
 [4] M. Fleischhauer, A. Imamoglu, and J. P. Marangos, *Rev. Mod. Phys.* **77**, 633 (2005).

- [5] N. V. Vitanov, A. A. Rangelov, B. W. Shore, and K. Bergmann, *Rev. Mod. Phys.* **89**, 015006 (2017).
- [6] B. W. Shore, *Adv. Opt. Photonics* **9**, 563 (2017).
- [7] J. Vanier, A. Godone, and F. Levi, *Phys. Rev. A* **58**, 2345 (1998).
- [8] S. Sevinçli, C. Ates, T. Pohl, H. Schempp, C. S. Hofmann, G. Günter, T. Amthor, M. Weidemüller, J. D. Pritchard, D. Maxwell *et al.*, *J. Phys. B* **44**, 184018 (2011).
- [9] M. Kasevich and S. Chu, *Phys. Rev. Lett.* **69**, 1741 (1992).
- [10] G. Morigi, J. Eschner, and C. H. Keitel, *Phys. Rev. Lett.* **85**, 4458 (2000).
- [11] A. Aspect, E. Arimondo, R. Kaiser, N. Vansteenkiste, and C. Cohen-Tannoudji, *J. Opt. Soc. Am. B* **6**, 2112 (1989).
- [12] J. Vanier, M. W. Levine, D. Janssen, and M. J. Delaney, *IEEE Trans. Instrum. Meas.* **52**, 822 (2003).
- [13] J. Vanier, *Appl. Phys. B* **81**, 421 (2005).
- [14] S. Guerandel, T. Zanon, N. Castagna, F. Dahes, E. de Clercq, N. Dimarcq, and A. Clairon, *IEEE Trans. Instrum. Meas.* **56**, 383 (2007).
- [15] T. A. Collaboration, J. Baron, W. C. Campbell, D. DeMille, J. M. Doyle, G. Gabrielse, Y. V. Gurevich, P. W. Hess, N. R. Hutzler, E. Kirilov *et al.*, *Science* **343**, 269 (2014).
- [16] A. Dantan, J. Cviklinski, E. Giacobino, and M. Pinard, *Phys. Rev. Lett.* **97**, 023605 (2006).
- [17] H. Schempp, G. Günter, C. S. Hofmann, C. Giese, S. D. Saliba, B. D. DePaola, T. Amthor, M. Weidemüller, S. Sevinçli, and T. Pohl, *Phys. Rev. Lett.* **104**, 173602 (2010).
- [18] C. Santori, P. Tamarat, P. Neumann, J. Wrachtrup, D. Fattal, R. Beausoleil, J. Rabeau, P. Olivero, A. Greentree, S. Prawer *et al.*, *Phys. Rev. Lett.* **97**, 247401 (2006).
- [19] W. R. Kelly, Z. Dutton, J. Schlafer, B. Mookerji, T. A. Ohki, J. S. Kline, and D. P. Pappas, *Phys. Rev. Lett.* **104**, 163601 (2010).
- [20] B. Michaelis, C. Emary, and C. W. J. Beenakker, *Europhys. Lett.* **73**, 677 (2006).
- [21] X. Xu, B. Sun, P. R. Berman, D. G. Steel, A. S. Bracker, D. Gammon, and L. J. Sham, *Nat. Phys.* **4**, 692 (2008).
- [22] M. Issler, E. M. Kessler, G. Giedke, S. Yelin, I. Cirac, M. D. Lukin, and A. Imamoglu, *Phys. Rev. Lett.* **105**, 267202 (2010).
- [23] C. G. Yale, B. B. Buckley, D. J. Christle, G. Burkard, F. J. Heremans, L. C. Bassett, and D. D. Awschalom, *Proc. Natl. Acad. Sci. USA* **110**, 7595 (2013).
- [24] C. M. Chow, A. M. Ross, D. Kim, D. Gammon, A. S. Bracker, L. J. Sham, and D. G. Steel, *Phys. Rev. Lett.* **117**, 077403 (2016).
- [25] G. Éthier-Majcher, D. Gangloff, R. Stockill, E. Clarke, M. Hugues, C. Le Gall, and M. Atatüre, *Phys. Rev. Lett.* **119**, 130503 (2017).
- [26] B. Rousseaux, D. Dzsoţjan, G. Colas des Francs, H. R. Jauslin, C. Couteau, and S. Guérin, *Phys. Rev. B* **93**, 045422 (2016).
- [27] Y. Han, J. Xiao, Y. Liu, C. Zhang, H. Wang, M. Xiao, and K. Peng, *Phys. Rev. A* **77**, 023824 (2008).
- [28] V. Ivanov and Y. Rozhdestvensky, *Phys. Rev. A* **81**, 033809 (2010).
- [29] Y. Gu, L. Wang, K. Wang, C. Yang, and Q. Gong, *J. Phys. B* **39**, 463 (2006).
- [30] F. T. Hioe and J. H. Eberly, *Phys. Rev. Lett.* **47**, 838 (1981).
- [31] J. Elgin, *Phys. Lett. A* **80**, 140 (1980).
- [32] J. R. Morris and B. W. Shore, *Phys. Rev. A* **27**, 906 (1983).
- [33] A. A. Rangelov, N. V. Vitanov, and B. W. Shore, *Phys. Rev. A* **74**, 053402 (2006).
- [34] B. W. Shore, *J. Mod. Opt.* **61**, 787 (2014).
- [35] G. S. V. N. V. Vitanov, [arXiv:1402.5673](https://arxiv.org/abs/1402.5673).
- [36] V. V. Albert and L. Jiang, *Phys. Rev. A* **89**, 022118 (2014).
- [37] G. Lindblad, *Commun. Math. Phys.* **48**, 119 (1976).
- [38] V. Gorini, A. Kossakowski, and E. C. G. Sudarshan, *J. Math. Phys.* **17**, 821 (1976).
- [39] H. Li, V. A. Sautenkov, Y. V. Rostovtsev, G. R. Welch, P. R. Hemmer, and M. O. Scully, *Phys. Rev. A* **80**, 023820 (2009).
- [40] B. Luo, H. Tang, and H. Guo, *J. Phys. B* **42**, 235505 (2009).
- [41] J. Cerrillo, A. Retzker, and M. B. Plenio, *Phys. Rev. Lett.* **104**, 043003 (2010).
- [42] J. Cerrillo, A. Retzker, and M. B. Plenio, *Phys. Rev. A* **98**, 013423 (2018).
- [43] M. B. Plenio and P. L. Knight, *Rev. Mod. Phys.* **70**, 101 (1998).
- [44] A. K. Patnaik, P. S. Hsu, G. S. Agarwal, G. R. Welch, and M. O. Scully, *Phys. Rev. A* **75**, 023807 (2007).
- [45] E. S. Kyoseva and N. V. Vitanov, *Phys. Rev. A* **73**, 023420 (2006).
- [46] E. A. Korsunsky and D. V. Kosachiov, *Phys. Rev. A* **60**, 4996 (1999).
- [47] W. Maichen, R. Gaggl, E. Korsunsky, and L. Windholz, *Europhys. Lett.* **31**, 189 (1995).
- [48] E. Arimondo, *Appl. Phys. B* **122**, 293 (2016).
- [49] M. Artoni and A. Zavatta, *Phys. Rev. Lett.* **115**, 113005 (2015).
- [50] H. Y. Ling, Y.-Q. Li, and M. Xiao, *Phys. Rev. A* **53**, 1014 (1996).
- [51] F. Renzoni, A. Lindner, and E. Arimondo, *Phys. Rev. A* **60**, 450 (1999).
- [52] F. Renzoni and E. Arimondo, *Opt. Commun.* **178**, 345 (2000).
- [53] H. Failache, L. Lenci, A. Lezama, D. Bloch, and M. Ducloy, *Phys. Rev. A* **76**, 053826 (2007).
- [54] J. Choi and D. S. Elliott, *Phys. Rev. A* **89**, 013414 (2014).
- [55] T. F. Havel, *J. Math. Phys.* **44**, 534 (2003).